

Lipidomic platform for structural identification of skin ceramides with α -hydroxyacyl chains

Zhexue Wu¹ · Jong Cheol Shon¹ · Doohyun Lee¹ · Kab-Tae Park¹ ·
Chang Seo Park² · Taeho Lee¹ · Hye Suk Lee³ · Kwang-Hyeon Liu¹

Received: 16 August 2015 / Revised: 2 November 2015 / Accepted: 1 December 2015 / Published online: 27 January 2016
© Springer-Verlag Berlin Heidelberg 2016

Abstract Skin ceramides are sphingolipids consisting of sphingoid bases, which are linked to fatty acids via an amide bond. Typical fatty acid acyl chains are composed of α -hydroxy fatty acid (A), esterified ω -hydroxy fatty acid (EO), non-hydroxy fatty acid (N), and ω -hydroxy fatty acid (O). We recently established a lipidomic platform to identify skin ceramides with non-hydroxyacyl chains using tandem mass spectrometry. We expanded our study to establish a lipidomic platform to identify skin ceramides with α -hydroxyacyl chains. Tandem mass spectrometry analysis of A-type ceramides using chip-based direct infusion nanoelectrospray-mass spectrometry showed the characteristic fragmentation pattern of both acyl and sphingoid units, which can be applied for structural identification of ceramides. Based on the tandem

mass spectrometry fragmentation patterns of A-type ceramides, comprehensive fragmentation schemes were proposed. Our results may be useful for identifying A-type ceramides in the stratum corneum of human skin.

Keywords Ceramide · Mass spectrometry · Skin lipid · Stratum corneum

Introduction

The stratum corneum (SC) is the outermost layer of the skin and acts as a barrier, protecting the organism against environmental influences [1, 2]. Its unique morphology consists of keratin-enriched corneocytes embedded in a mixture of lipids containing ceramides, cholesterol, free fatty acids, phospholipids, and triacylglycerol [3, 4]. Among these skin lipids, ceramides are the most important lipid metabolites for the permeability barrier function as well as for the water-holding capacity of the skin [5]. The ceramide profiles in human SC were reported to be altered in atopic dermatitis, allergic contact dermatitis, and psoriasis [6–9].

Ceramides are sphingolipids composed of a sphingoid base linked to fatty acids through an amide linkage. Sphingoid units include dihydrosphingosine (dS), 6-hydroxysphingosine (H), sphingosine (S), and phytosphingosine (P), while free fatty acid units include α -hydroxylated (A), non-hydroxylated (N), and ω -hydroxylated (O), of which the ω -hydroxyacyl chain can be esterified to a fatty acid (E) [10]. In general, the carbon chain number of the amide-linked fatty acid varies from C16 to C40, while that of the sphingoid base varies from C12 to C22, though C18 is the most common [11]. Among the four types of fatty acid units, A- and N-type ceramides are abundant in the human stratum corneum (Fig. 1) [12].

Zhexue Wu, Jong Cheol Shon and Doohyun Lee contributed equally to this work.

Electronic supplementary material The online version of this article (doi:10.1007/s00216-015-9239-4) contains supplementary material, which is available to authorized users.

✉ Hye Suk Lee
sianalee@catholic.ac.kr

✉ Kwang-Hyeon Liu
dstlkh@gmail.com

¹ BK21 Plus KNU Multi-Omics based Creative Drug Research Team, College of Pharmacy and Research Institute of Pharmaceutical Sciences, Kyungpook National University, 80 Daehak-ro, Buk-gu, Daegu 702-701, Republic of Korea

² Department of Chemical and Biochemical Engineering, Dongguk University, 26 Pil-dong 3-ga, Jung-gu, Seoul 100-715, Republic of Korea

³ College of Pharmacy and Integrated Research Institute of Pharmaceutical Sciences, The Catholic University of Korea, 43-1 Yeokgok 2-dong, Wonmi-gu, Bucheon 420-743, Republic of Korea

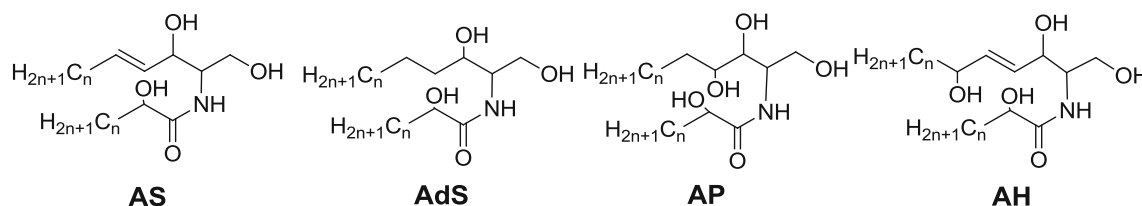


Fig. 1 Structure of four AS-, AdS-, AP-, and AH-type ceramide species

Several analytical platforms, including high-performance thin-layer chromatography [13–16], high-performance liquid chromatography [17, 18], gas chromatography/mass spectrometry (MS) [16, 19], and liquid chromatography-tandem mass spectrometry [11, 12, 20, 21], have been used to analyze skin ceramides. Recently, direct infusion-tandem mass spectrometry was used for shotgun analysis of ceramides, phospholipids, and triacylglycerols [22, 23]. We also established a lipidomic platform for the identification of N-type skin ceramides using direct infusion-tandem mass spectrometry [24]. Currently, the mass fragmentation patterns and the structure of each fragment ion of four ceramides having α -hydroxy fatty acids have not been completely elucidated.

In this study, we characterized the tandem mass spectrometry (MS/MS) fragmentation pattern of four ceramides having α -hydroxy fatty acids by examining their product ion scan mass spectra. We also developed a method for identifying and profiling A-type ceramides in the human stratum corneum using chip-based direct infusion nanoelectrospray-tandem mass spectrometry.

Experimental

Reagents

Ammonium acetate, chloroform, dimethylformamide, ethyl acetate (EtOAc), imidazole, 1-ethyl-3-(3-dimethylaminopropyl)carbodiimide (EDCI), 1-hydroxybenzotriazole (HOBt), 2,6-lutidine, methanol, *D-ribo*-phytosphingosine, *tert*-butyldimethylsilyl chloride (TBSCl), tetrabutylammonium fluoride (TBAF), tetrahydrofuran (THF), and trimethylsilyl trifluoromethanesulfonate (TBSOTf) were purchased from Sigma Chemical Co. (St. Louis, MO, USA). Synthetic ceramides CER[A(20:0)S(18:1)], CER[A(22:0)S(18:1)], CER[A(16:0)dS(18:0)], and CER[A(18:0)dS(18:0)] were obtained from Avanti Polar Lipids (Alabaster, AL, USA) or Matreya (Pleasant Gap, PA, USA).

Synthesis of CER[AP] standards (Scheme 1)

General procedure for fatty acid 2

To a solution of 2-hydroxy fatty acid **1** (1.0 equiv.) in dimethylformamide (0.1 M) at 0 °C, we added imidazole

(3.0 equiv.) and TBSCl (3.0 equiv.). The reaction mixture was stirred at room temperature for 6 h, diluted with EtOAc, and washed with 1 N HCl. The organic layer was dried over MgSO₄ and concentrated under reduced pressure. The crude mixture was dissolved in 0.2 M methanol. This solution was cooled down to 0 °C and K₂CO₃ (2.0 equiv.) and H₂O (one third of methanol) were added. After overnight incubation at room temperature, the solvent was removed in vacuo. The residue was diluted with H₂O and acidified to pH 4 by addition of 1 N HCl. The resultant mixture was diluted with EtOAc, washed with H₂O, dried over MgSO₄, filtered, and concentrated in vacuo to give the desired acid **2**, which was used in the next step without further purification.

((6S,7S,8R)-7-((tert-Butyldimethylsilyloxy)-2,2,3,3,10,10,11,11-octamethyl-8-tetradecyl-4,9-dioxo-3,10-disiladodecan-6-amine (4)

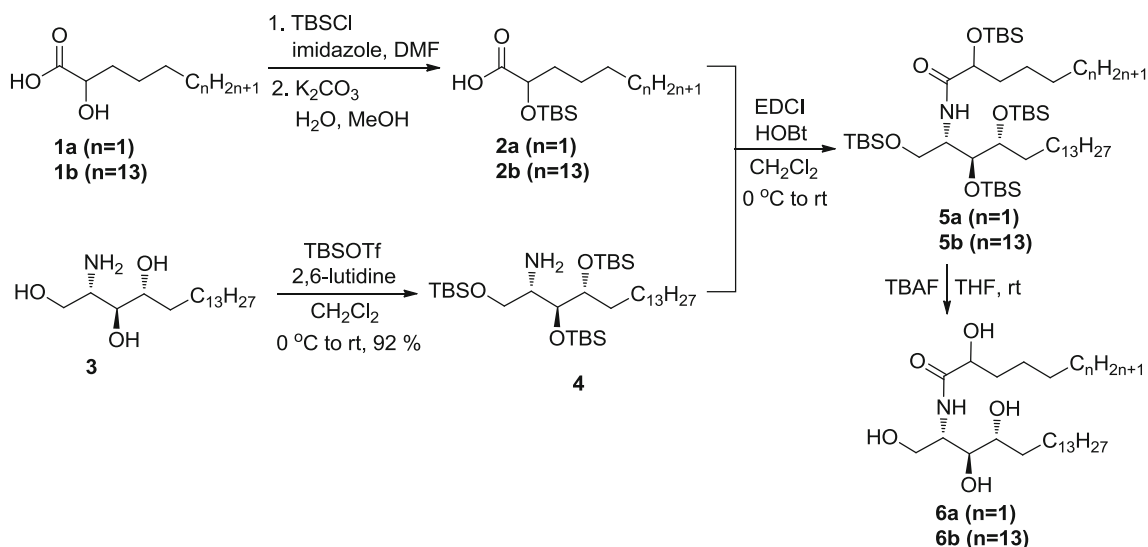
We added 2,6-lutidine (3.00 mL, 25.5 mmol) and TBSOTf (2.34 mL, 10.2 mmol) to a solution of *D-ribo*-phytosphingosine (**3**, 635 mg, 2.00 mmol) in CH₂Cl₂ (20 mL) at 0 °C. The reaction mixture was stirred at room temperature for 3 h. The reaction was quenched with methanol at 0 °C, and then the resultant mixture was diluted with EtOAc, washed with H₂O, dried (MgSO₄), filtered, and concentrated under reduced pressure. Purification of the residue using flash silica gel column chromatography (hexane/EtOAc, 20:1) resulted in the silyl-protected phytosphingosine **4** (1.21 g, 92 %) as a pale yellow oil.

General procedure for silyl protected ceramide 5

EDCI (1.60 equiv), HOBt (1.30 equiv), and fatty acids (1.30 equiv) were added to a stirred solution of **4** in CH₂Cl₂ (0.02 M). The reaction mixture was stirred under argon for 6 h. The solvent was removed in vacuo, and the resulting residue was purified by flash column chromatography (hexane/EtOAc, 20:1) to afford the desired silyl-protected ceramide derivative **5**.

General procedure for ceramide 6

To a solution of **5** in THF (0.02 M), we added TBAF (6.00 equiv., 1.0 M solution in THF). The solution was stirred for 6 h at room temperature, followed by quenching with aqueous saturated NH₄Cl and extracted twice with EtOAc. The



Scheme 1 Synthesis of CER[AP] standards

combined organic layers were dried over MgSO₄, filtered, and concentrated under reduced pressure. The residue was purified by flash silica gel column chromatography to afford the desired ceramide derivative **6**.

2-Hydroxy-N-((2S,3S,4R)-1,3,4-trihydroxyoctadecan-2-yl)hexanamide (ceramide A(6:0)P(18:0), 6a)

Less polar diastereomer of **6a** is as follows: white solid, yield 32 %, ¹H NMR (500 MHz, C₅D₅N) δ 8.60 (d, *J*=8.8 Hz, 1H), 7.49 (d, *J*=5.3 Hz, 1H), 6.75 (s, 1H), 6.62 (d, *J*=6.5 Hz, 1H), 6.20 (d, *J*=6.2 Hz, 1H), 5.15–5.08 (m, 1H), 4.62–4.50 (m, 2H), 4.50–4.43 (m, 1H), 4.37–4.24 (m, 2H), 2.29–2.15 (m, 2H), 2.04–1.84 (m, 3H), 1.78–1.59 (m, 3H), 1.48–1.15 (m, 24H), 0.86 (t, *J*=6.9 Hz, 3H), and 0.81 (t, *J*=7.4 Hz, 3H). More polar diastereomer of **6a** is the following: white solid, yield 29 %, ¹H NMR (500 MHz, C₅D₅N) δ 8.57 (d, *J*=8.9 Hz, 1H), 6.67 (br s, 1H), 5.30–4.70 (m, 4H), 4.59 (dd, *J*=7.8, 3.7 Hz, 1H), 4.52 (dd, *J*=10.7, 4.5 Hz, 1H), 4.43 (dd, *J*=10.8, 5.0 Hz, 1H), 4.37–4.25 (m, 2H), 2.33–2.16 (m, 2H), 2.05–1.86 (m, 3H), 1.79–1.58 (m, 3H), 1.51–1.18 (m, 24H), 0.86 (t, *J*=7.0 Hz, 3H), and 0.83 (t, *J*=7.4 Hz, 3H).

2-Hydroxy-N-((2S,3S,4R)-1,3,4-trihydroxyoctadecan-2-yl)octadecanamide (ceramide A(18:0)P(18:0), 6b)

Ceramide 6b is as follows: white solid, yield 82 %, diastereomeric ratio=7:3 (assigned by the integral ratio of ¹H NMR spectrum), ¹H NMR (500 MHz, C₅D₅N) δ 8.63 (d, *J*=8.8 Hz, 0.7H), 8.58 (d, *J*=8.8 Hz, 0.3H), 5.70–4.800 (m, 5H), 4.63 (dd, *J*=7.7, 3.5 Hz, 1H), 4.57–4.41 (m, 2H), 4.39–4.25

(m, 2H), 2.30–2.20 (m, 2H), 2.10–1.86 (m, 3H), 1.86–1.60 (m, 3H), 1.52–1.17 (m, 48H), and 0.87 (t, *J*=6.7 Hz, 6H).

Ceramide analysis and data processing

The human stratum corneum samples used in our previous study [24] were used in A-type ceramide identification. All individuals were enrolled with informed consent. Ceramide profiling was performed on an LTQ XL mass spectrometer (Thermo Scientific, Waltham, MA, USA) equipped with a chip-based nanoelectrospray infusion system (TriVersa, Advion Biosciences, Ithaca, NY, USA) as previously described [24]. Briefly, each sample was infused into an ion source for 2 min. The data collection involved a full scan and data-dependent MS/MS scan. Ceramides having α-hydroxy fatty acids were identified based on their characteristic mass fragmentation patterns.

Results and discussion

MS/MS analysis of A-type ceramides

MS/MS analysis of A-type ceramides was performed similarly to that used for N-type ceramides [24]. The targeted product ion scan mass spectra obtained from the Nanomate-LTQ system provided characteristic fragmentation patterns for both the acyl and sphingoid chains, which were used for structural identification of A-type ceramides (see [Electronic Supplementary Material, ESM](#)). The identification procedures for synthetic ceramide standards [A(20:0)S(18:1) (AS, MW=609)], [A(18:0)dS(18:0) (AdS, MW=583)], and [A(18:0)P(18:0) (AP, MW=599)] were as follows: AH-type ceramide (ceramide class consisting of α-hydroxy fatty acids

and 6-hydroxy-4-sphingene) is commercially unavailable; therefore, the fragmentation pattern of this ceramide was predicted based on the product ion scan mass spectrum pattern of A(24:0)H(18:1) ceramide (AH, MW=681), which is normally found in the human stratum corneum [12]. A-type ceramide

species were found as acetate adducts similar to N-type ceramides [24] because the ammonium acetate existed in the constitution solvent mixture. The product ion scan mass spectra of these adducts gave deprotonated molecular ions $[M-H]^-$. Product ion scan spectra of these

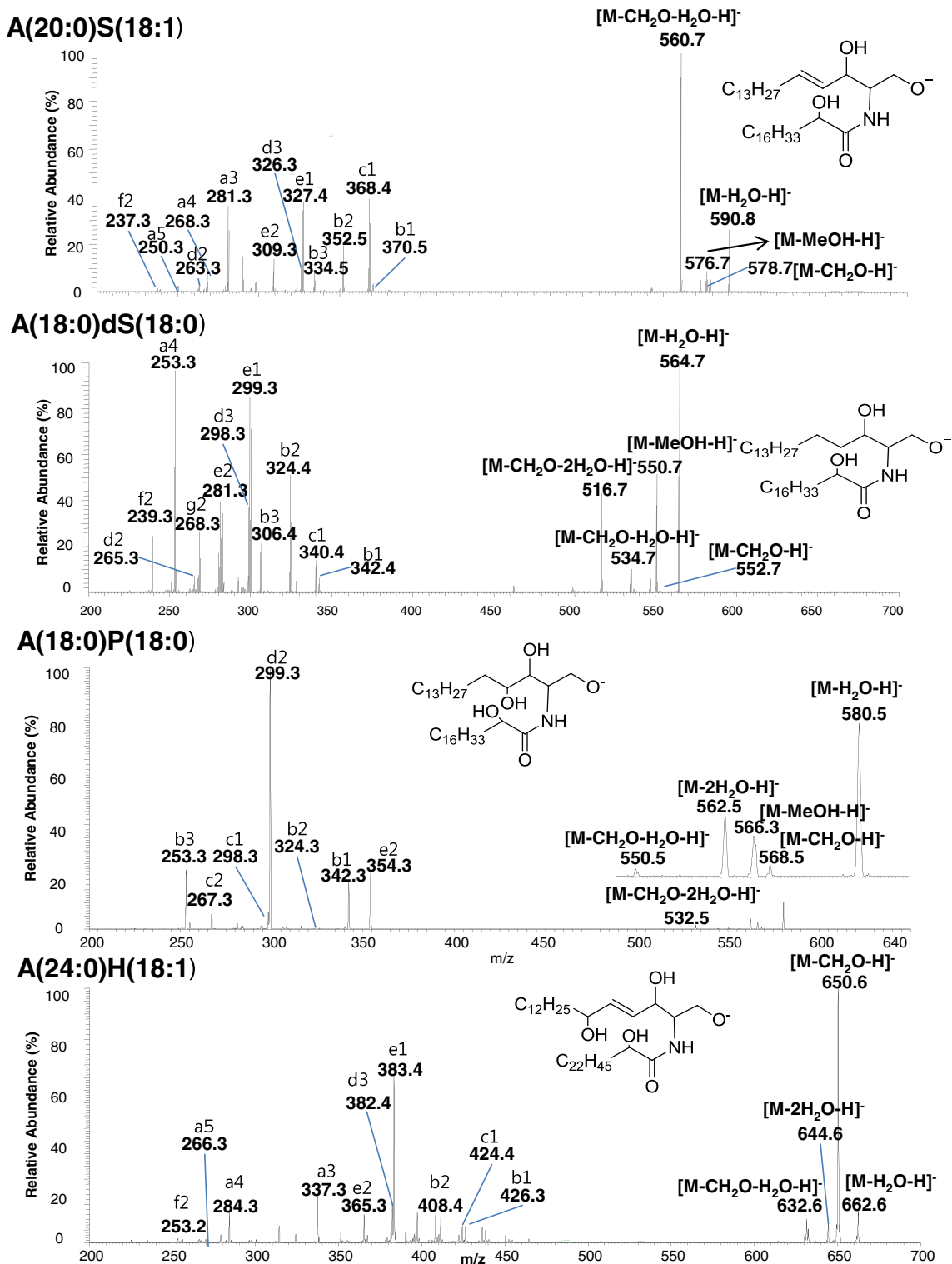
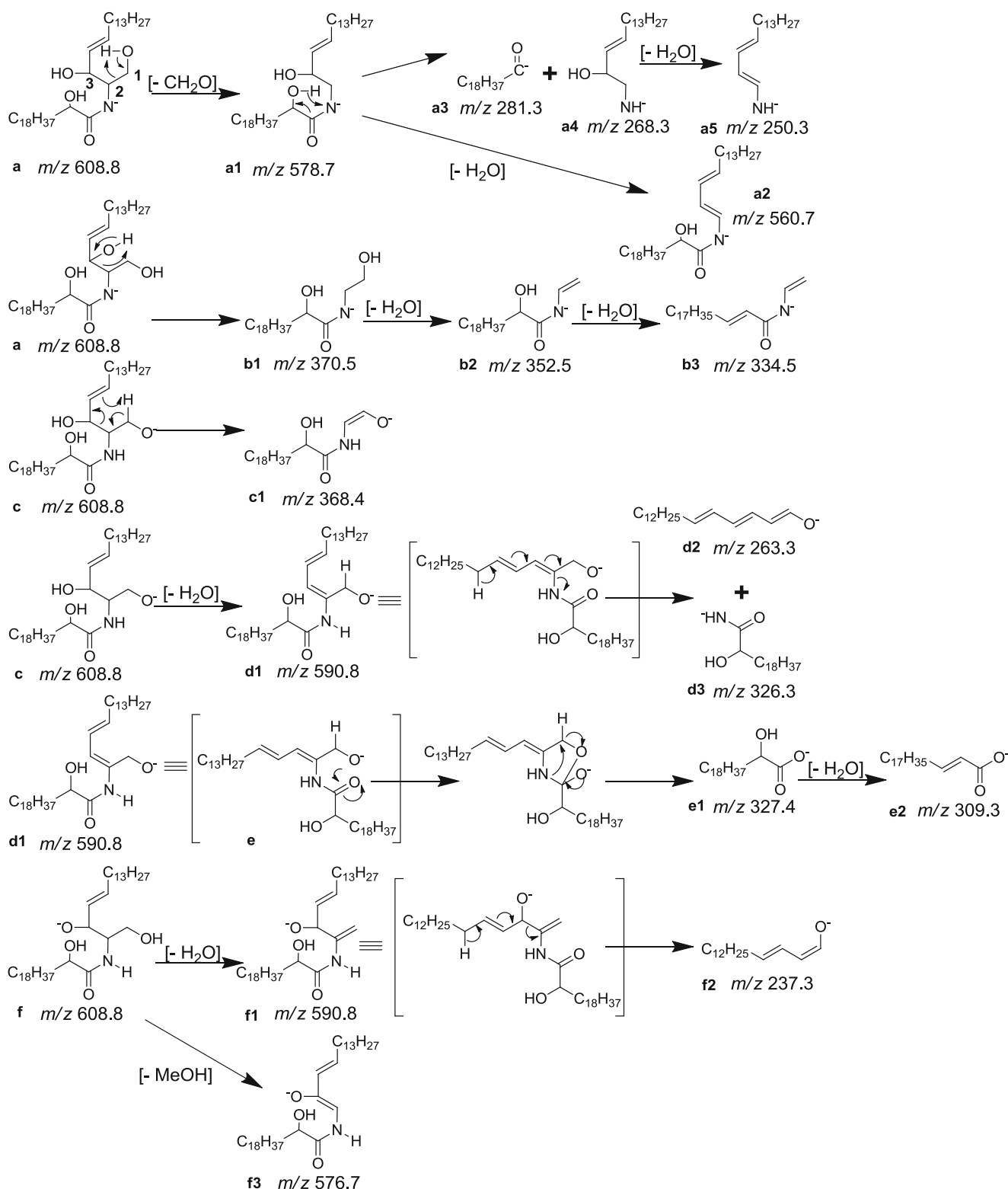


Fig. 2 Tandem mass spectra of ceramides [A(20:0)S(18:1)], [A(18:0)dS(18:0)], [A(18:0)P(18:0)], and [A(24:0)H(18:1)]

pseudo-molecular ions generated valuable fragmentation information for the identification of AS-type (ceramide class consisting of α -hydroxy fatty acids and 4-sphinganine), AdS-type (ceramide class consisting of

α -hydroxy fatty acids and sphinganine), AP-type (ceramide class consisting of α -hydroxy fatty acids and 4-hydroxysphinganine), and AH-type ceramide species (Fig. 2).

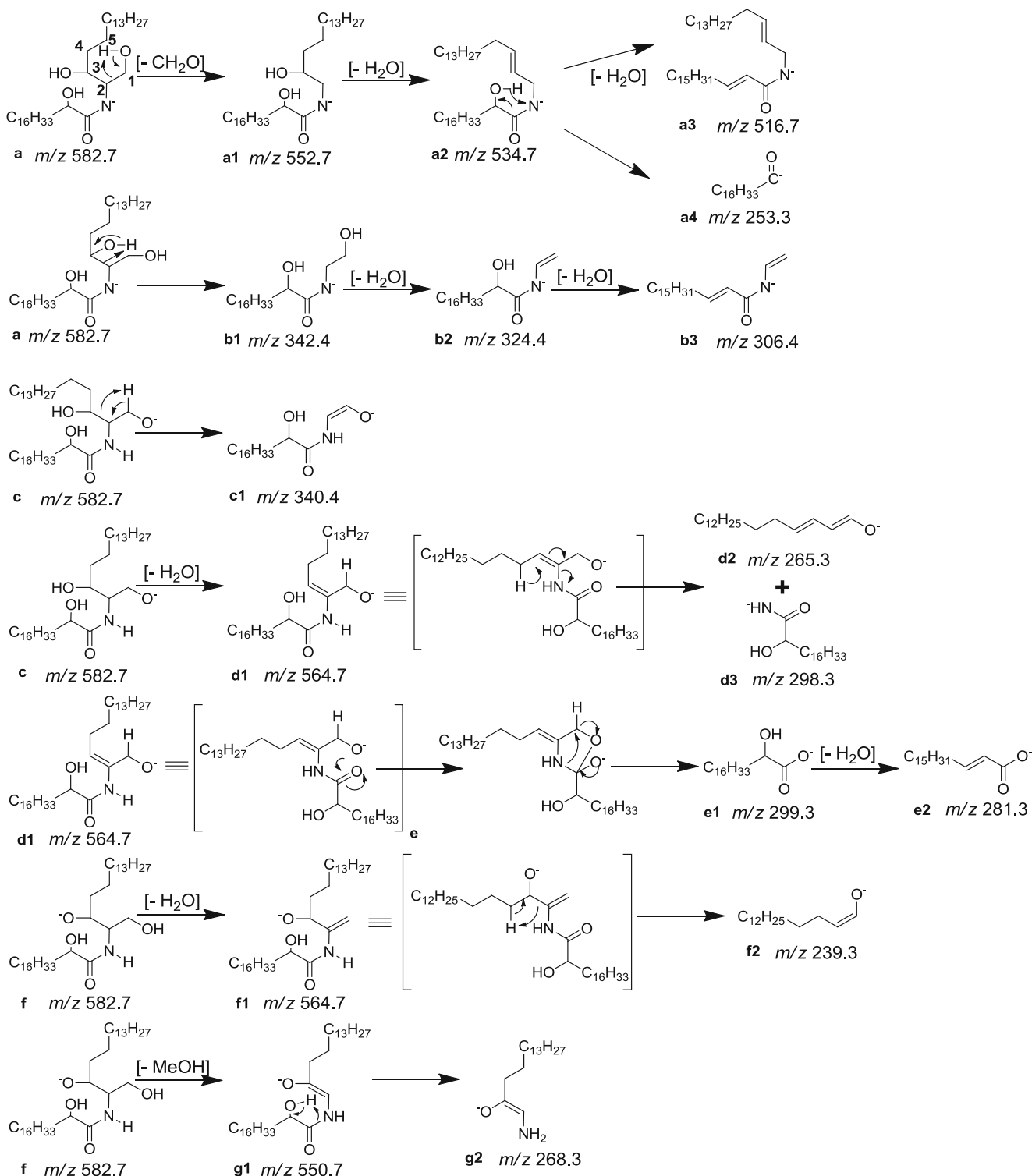


Scheme 2 Suggested fragmentation pathways of CER[AS] standard [A(20:0)S(18:1)] by means of collision-induced dissociation in negative ion mode

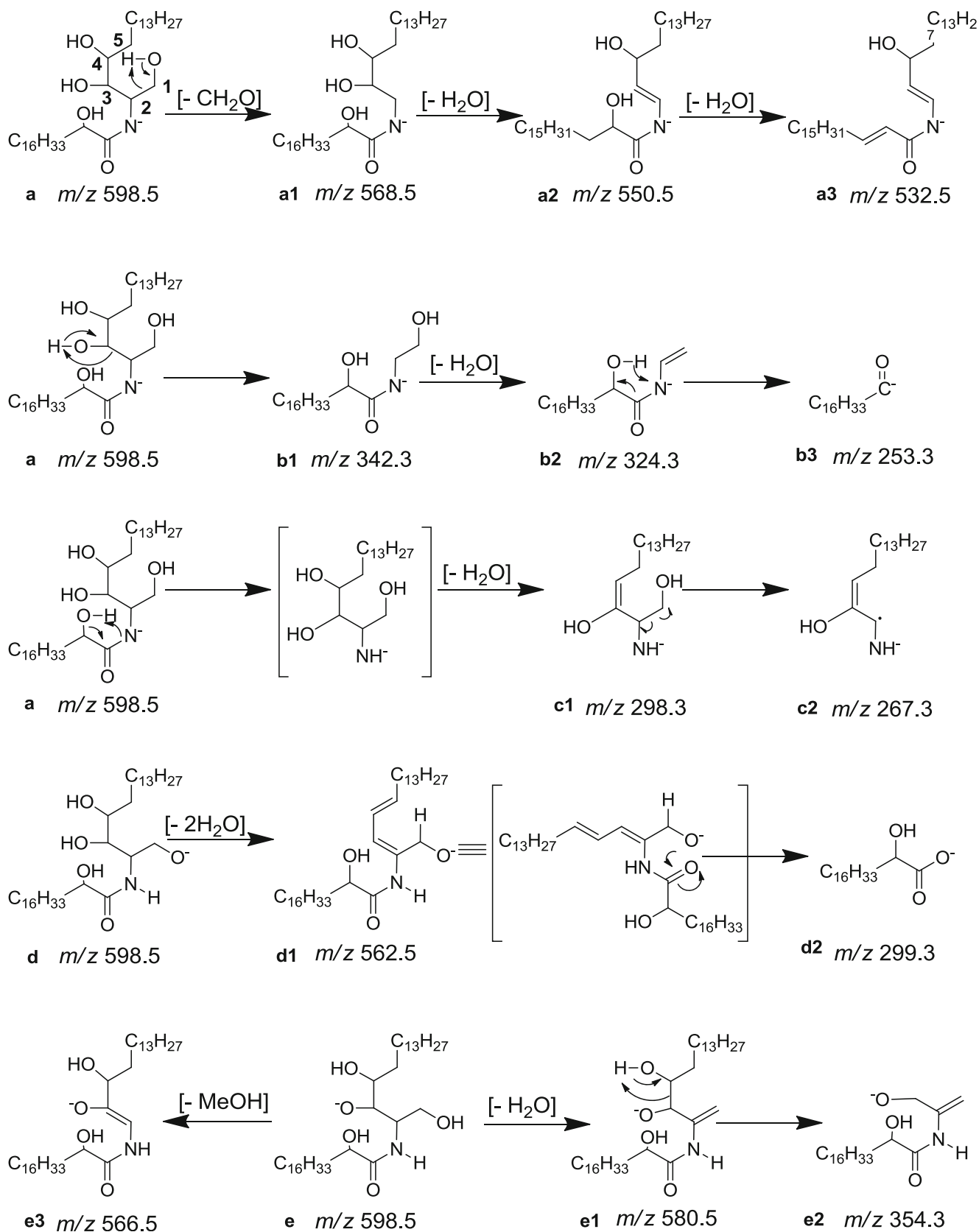
Characterization of mass fragmentation pattern of AS-type ceramide

The suggested fragmentation pathway of the ceramide consisting of α -hydroxy fatty acids and 4-sphinganine (AS-

type) is illustrated in Scheme 2. These characteristic fragmentation patterns can be used to identify AS-type ceramide species with different fatty acids. The product ion scan mass spectrum of ceramide A(20:0)S(18:1), which was obtained by fragmenting the deprotonated molecular ion $[M-H]^-$ with



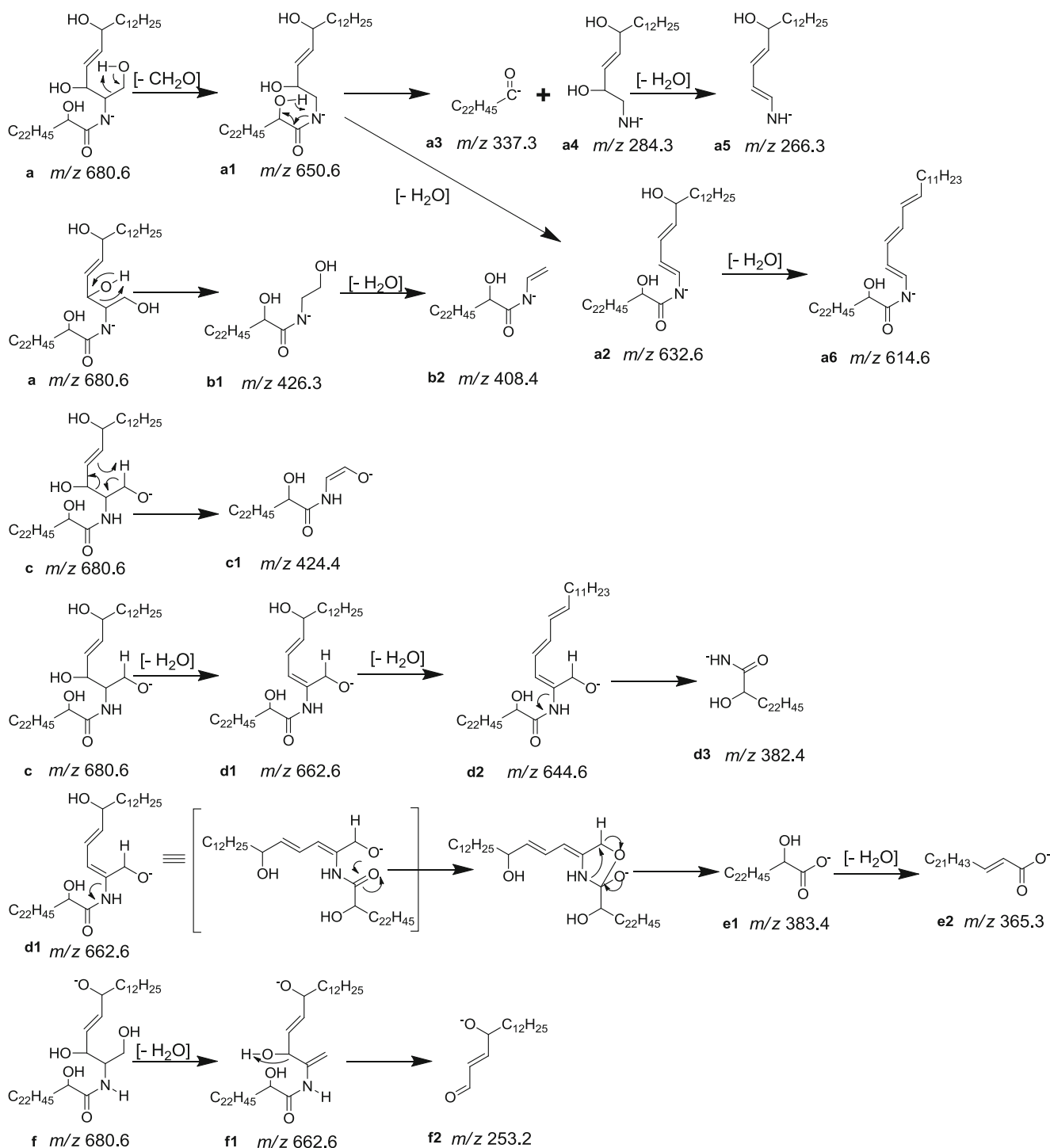
Scheme 3 Suggested fragmentation pathways of CER[AdS] standard [A(18:0)dS(18:0)] by means of collision-induced dissociation in negative ion mode



Scheme 4 Suggested fragmentation pathways of CER[AP] standard [A(18:0)P(18:0)] by means of collision-induced dissociation in negative ion mode

m/z 608.8 through collision, yielded a fragment ion at m/z 578.7 (the loss of CH_2O moiety, **a1**); cleavage induced the formation of ions, with the charge retained at the fatty acyl and sphingoid moiety with m/z 281.3 (**a3**) and 268.3 (**a4**), respectively. AS-type ceramide also lost both the CH_2O group and water, resulting in an abundant fragment ion at m/z 560.7 (**a2**). Cleavage at the C2–C3 bond (see structure **a** in Scheme 2

for numbering of carbon atoms) resulted in a characteristic ion at m/z 370.5 (**b1**) which has the charge on the fatty acid unit, and the subsequent loss of water resulted in fragment ions at m/z 352.5 (**b2**) and 334.5 (**b3**). Cleavage at the C2–C3 bond from pseudomolecular ion **c** led to a fragment ion at m/z 368.4 (**c1**) which has the charge on the fatty acyl unit. A loss of a water molecule could occur at two different positions (**c** and **f**)



Scheme 5 Suggested fragmentation pathways of CER[AH] standard [A(24:0)H(18:1)] by means of collision-induced dissociation in negative ion mode

and occurred with double bond formation (m/z 590.8, **d1** and **f1**). One double bond could be formed between C2 and C3 (**d1**), and subsequent cleavage at this location resulted in fragment ions at m/z 263.3 (**d2**) and 326.3 (**d3**), with charges on the sphingoid and fatty acyl moiety, respectively. With a double bond at this position, further rearrangement (**e**) can take place, resulting in a fragment ion at m/z 327.4 (**e1**), which is the α -hydroxy fatty acid itself; a subsequent loss of water resulted in a fragment ion at m/z 309.3 (**e2**). A second possible position was located between C1 and C2 (**f1**), and cleavage at this position resulted in a fragment ion (m/z 237.3) which has a charge on the sphingoid unit (**f2**). Ceramide A(20:0)S(18:1) also showed a fragment ion at m/z 576.7 (loss of CH₃OH moiety, **f3**).

Several fragments related to the fatty acyl chain were observed including **a3**, **b2**, **c1**, **d3**, **e1**, and **e2**. Furthermore, **a4**, **a5**, and **f2** were fragment ions related to sphingoid unit. These results were consistent with the findings of Han [25], Hsu and Turk [26], t'Kindt et al. [12], Shin et al. [24], and Vietzke et al. [14].

Characterization of mass fragmentation pattern of AdS-type ceramide

The proposed fragmentation pathway of the ceramide consisting of α -hydroxy fatty acids and sphinganine (AdS-type) is illustrated in Scheme 3 and described below. The MS/MS spectrum of the ceramide A(18:0)dS(18:0) standard, which was obtained by fragmenting the pseudomolecular ion with m/z 582.7, yielded a fragment ion at m/z 552.7 (loss of CH₂O group, **a1**); the subsequent loss of water resulted in fragment ions at m/z 534.7 (**a2**) and 516.7 (**a3**). A fragment ion at m/z 534.7 (**a2**) induced the formation of an ion with m/z 253.3 (**a4**). Cleavage at the C2–C3 bond (see structure **a** in Scheme 3 for numbering of carbon atoms) resulted in a fragment ion at m/z 342.4 (**b1**) which has the charge on the fatty acyl unit, and the subsequent loss of water resulted in fragment ions at m/z 324.4 (**b2**) and 306.4 (**b3**). Cleavage at the C2–C3 bond from pseudomolecular ion **c** also resulted in a fragment ion at m/z 340.4 (**c1**) which has the charge on the fatty acyl unit. A neutral loss of a water molecule could occur at two different positions (**c** and **f**) with a double bond formation (m/z 564.7, **d1** and **f1**). One double bond could be formed between C2 and C3 (**d1**), and subsequent cleavage at this location resulted in fragment ions at m/z 265.3 (**d2**) and 298.3 (**d3**) with the charge on the sphingoid and fatty acyl unit, respectively. With a double bond at this position (**d1**), further rearrangement (**e**) could take place, resulting in a fragment ion at m/z 299.3 (**e1**), which is the α -hydroxy fatty acid itself, while the subsequent loss of a water molecule results in a fragment ion at m/z 281.3 (**e2**). A second possible position was located between C1 and C2 (**f1**), and cleavage at this location resulted in a fragment ion with m/z 239.3 (**f2**) which

has the charge on the sphingoid unit. Ceramide A(18:0)dS(18:0) also showed a fragment ion at m/z 550.7 (loss of CH₃OH group, **g1**), and cleavage induced the formation of an ion with the charge retained at the sphingoid base with m/z 268.3 (**g2**).

Several fragments related to the fatty acyl chain were observed, including **a3**, **b2**, **b3**, **c1**, **e1**, and **e2**. Furthermore, **f2** and **g2** were fragments related to sphingoid unit. These results agree with the findings of t'Kindt et al. [12] and Shin et al. [24].

Characterization of mass fragmentation pattern of AP-type ceramide

The MS/MS spectrum of phytoceramide A(18:0)P(18:0) generated by fragmenting the pseudomolecular ion [M-H]⁻ with m/z 598.5 (**a**) through collision revealed an informative fragmentation pattern. Ceramide A(18:0)P(18:0) showed a fragment ion at m/z 568.5 (loss of CH₂O group, **a1**), and the subsequent loss of water resulted in fragment ions at m/z 550.5 (**a2**) and 532.5 (**a3**). Cleavage at the C2–C3 bond (see structure **a** in Scheme 4 for numbering of carbon atoms) resulted in a characteristic ion at m/z 342.4 (**b1**) which has the charge on the fatty acyl chain, and the subsequent loss of water

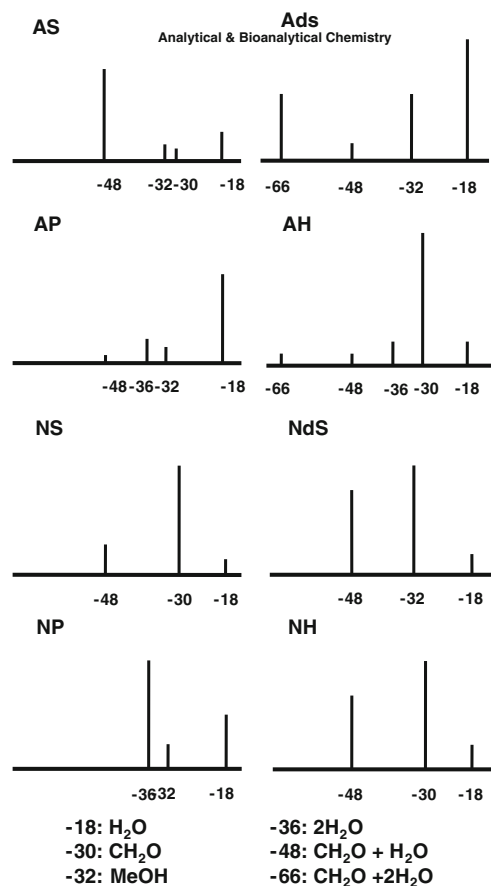


Fig. 3 General MS/MS fragmentation patterns of A-type ceramides and N-type ceramides

resulted in a fragment ion at m/z 324.3 (**b2**). A fragment ion at m/z 324.3 (**b2**) induced the formation of an ion with m/z 253.3 (**b3**). AP-type ceramide also showed cleavage of the fatty acyl chain, and this fragment ion showed a neutral loss of water

(**c1**, m/z 298.3) and further loss of a CH_2OH radical (**c2**, m/z 267.3). The loss of a water molecule could occur at two different positions (**d** and **e**) with the formation of a double bond (m/z 580.5 and 562.5). Loss of two water molecules resulted

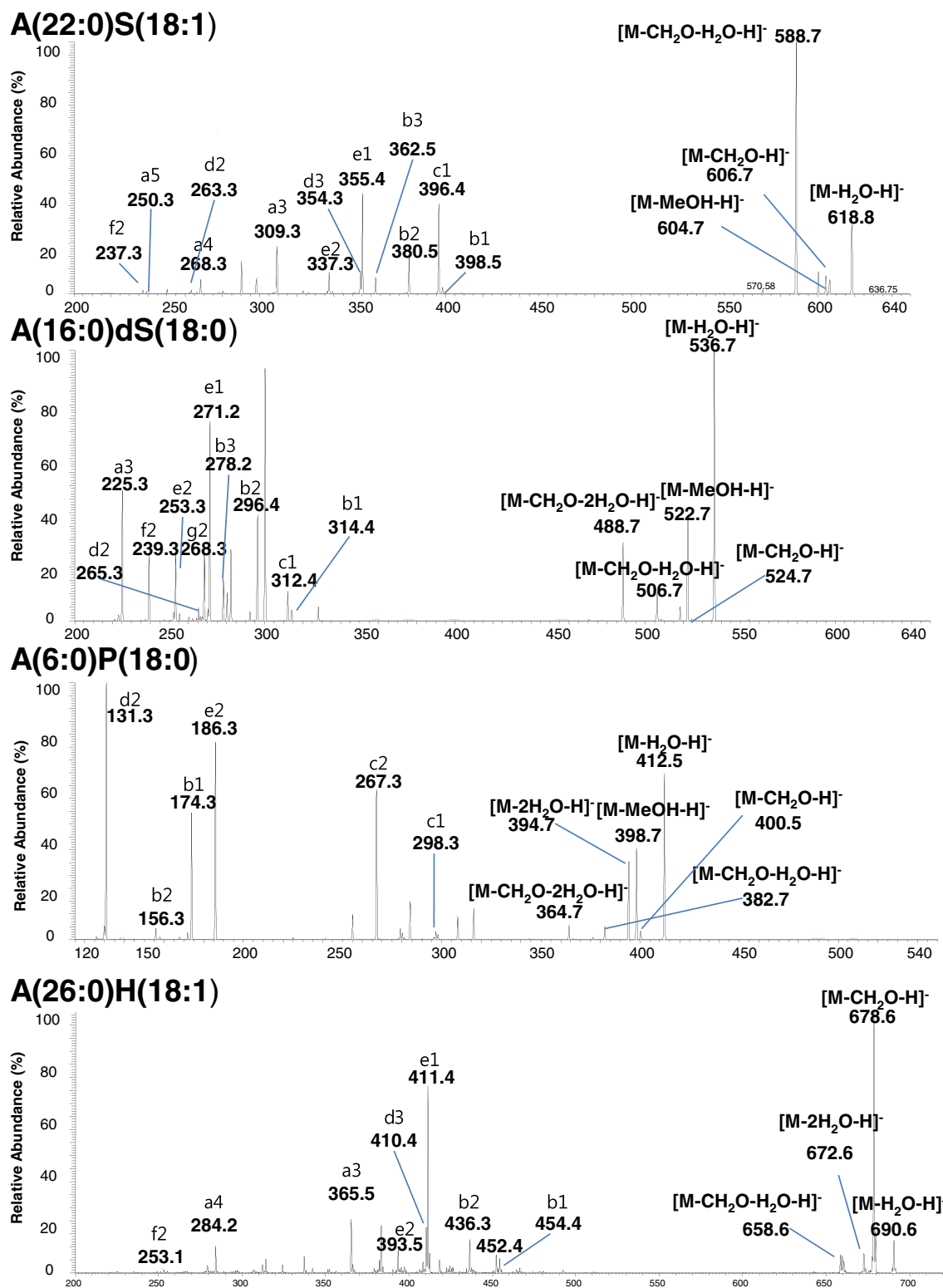


Fig. 4 Tandem mass spectra of ceramides [A(22:0)S(18:1)], [A(16:0)dS(18:0)], [A(6:0)P(18:0)], and [A(26:0)H(18:1)]

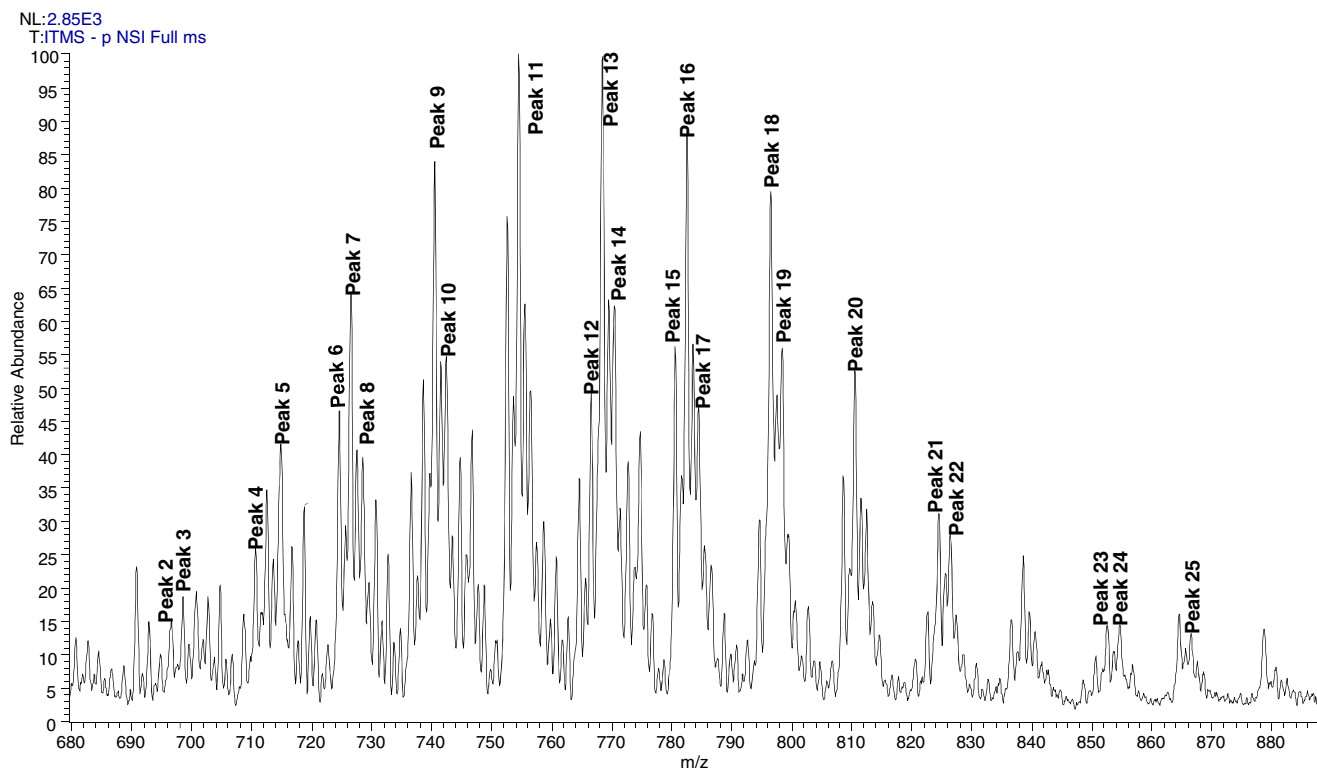


Fig. 5 Typical mass spectrum of the ceramide extracts from the stratum corneum of human skin using electrospray ionization in negative ion mode (The peak information is in Table 1)

in the formation of two double bonds at the C2–C3 and C4–C5 bonds (**d1**, m/z 562.5), and subsequent rearrangement could have resulted in a fragment ion at m/z 299.3 (**d2**), which is the α -hydroxy fatty acid itself. A second possible position was located between C1 and C2 (**e1**), and cleavage at this location resulted in a fragment ion with m/z 354.3 (**e2**) which has the charge on the fatty acyl chain. Ceramide AP (**e**) also showed abundant fragment ion at m/z 566.5 (loss of CH_3OH group, **e3**).

Several fragments related to the fatty acyl chain were observed, including **b2**, **b3**, **d3**, **e1**, and **e2**. Furthermore, **c1** and **c2** were fragment ions related to the sphingoid unit. These results agree with the findings of t'Kindt et al. [12], Shin et al. [24], and Vietzke et al. [14].

Characterization of mass fragmentation pattern of AH-type ceramide

AH-type ceramide is not commercially available; therefore, the fragmentation pattern of this ceramide was proposed based on the MS/MS spectrum of A(24:0)H(18:1) (MW=681), which is found in the human skin. The proposed fragmentation pathway of AH type ceramide is illustrated in Scheme 5 and described below. The MS/MS spectrum of the ceramide A(24:0)H(18:1) by fragmenting the pseudomolecular ion $[\text{M}-\text{H}]^-$ with m/z 680.5 (**a**) through collision yielded informative fragment ions at

m/z 650.6 (loss of CH_2O group, **a1**) and 632.6 (loss of CH_2O and H_2O group, **a2**). A fragment ion at m/z 650.6 (**a1**) induced the formation of ions, with the charge on the fatty acyl and sphingoid unit as m/z 337.3 (**a3**) and 284.3 (**a4**), respectively. The subsequent loss of a water molecule from m/z 284.3 (**a4**) resulted in a fragment ion at m/z 266.3 (**a5**). Cleavage at the C2–C3 bond (see structure **a** in Scheme 5 for numbering of carbon atoms) resulted in a characteristic ion at m/z 426.3 (**b1**), which has the charge on the fatty acyl unit, and the subsequent loss of water resulted in a fragment ion at m/z 408.4 (**b2**). Cleavage at the C2–C3 bond from pseudomolecular ion **c** led to a characteristic ion at m/z 424.4 (**c1**) which has the charge on the fatty acyl unit. The neutral loss of a water molecule occurred at two different positions (**c** and **f**) with double bond formation (m/z 662.6). One double bond was formed between C2 and C3 (**d1**), and subsequent cleavage at this location resulted in a fragment ion at m/z 382.4 (**d3**), which has the charge on the fatty acyl unit. With a double bond at this position, further rearrangement (**e**) occurred, resulting in a fragment ion at m/z 383.4 (**e1**), which is the α -hydroxy fatty acid itself, and the subsequent loss of water molecule resulted in a fragment ion at m/z 365.3 (**e2**). A second possible position was located between C1 and C2 (**f1**), and cleavage at this position resulted in a fragment ion with m/z 253.2 (**f2**), which has charge on the sphingoid unit.

Table 1 Identification of A-type ceramides which are found in human stratum corneum

No.	MW	[M-H] ⁻	[M+CH ₃ COO] ⁻	Identified ceramides				
				Abundance	Type	Total carbon	Acyl chain	Sphingoid base
1	555.6	554.6	614.6	Major	AH	33:1	16:0	17:1
				Minor	AdS	34:0	16:0	18:0
				Minor	NP	34:0	16:0	18:0
2	637.6	636.6	696.6		AS	40:1	22:0	18:0
3	639.6	638.6	698.6	Major	AH	39:1	21:0	18:1
				Minor	NP	40:0	22:0	18:0
							24:0	16:0
4	651.6	650.6	710.6		AS	41:1	24:0	17:1
5	655.6	654.6	714.6		AP	40:0	23:0	17:0
6	665.6	664.6	724.6		AS	42:1	24:0	18:1
7	667.6	666.6	726.6	Major	AH	41:1	23:0	18:1
							25:0	16:1
				Minor	NP	42:0	24:0	18:0
8	669.6	668.6	728.6		AP	41:0	23:0	18:0
							21:0	20:0
							25:0	16:0
9	681.6	680.6	740.6	Major	AH	42:1	24:0	18:1
							23:0	19:1
				Minor	NP	43:0	25:0	18:0
10	683.6	682.6	742.6		AP	44:0	24:0	18:0
							25:0	17:0
							25:0	17:0
11	695.6	694.6	754.6	Major	AH	43:1	25:0	18:1
				Minor	NP	44:0	24:0	20:0
							24:0	20:0
12	707.6	706.6	766.6		AS	45:1	25:0	20:1
13	709.6	708.6	768.6	Major	NP	44:0	27:0	18:0
							28:0	17:0
							25:0	20:0
14	711.6	710.6	770.6	Minor	AH	44:1	26:0	18:1
					AP	44:0	24:0	20:0
							26:0	18:0
15	721.6	720.6	780.6	Major	AS	46:1	26:0	20:1
				Minor	NH	46:1	26:0	20:1
				Major	AH	45:1	25:0	20:1
16	723.6	722.6	782.6				26:0	19:1
				Minor	NP	46:0	28:0	18:0
					AP	45:0	25:0	20:0
17	725.6	724.6	784.6		AP	45:0	25:0	20:0
18	737.6	736.6	796.6	Major	AH	46:1	26:0	20:1
							24:0	22:1
				Minor	NP	47:0	29:0	18:0
19	739.6	738.6	798.6		AP	46:0	24:0	22:0
				Major	AH	47:1	27:0	20:1
							25:0	22:1
20	751.6	750.6	810.6				30:0	18:0
				Minor	NP	48:0	30:0	18:0
				Major	AH	48:1	28:0	20:1
21	765.6	764.6	824.6	Major	AH	48:1	28:0	20:1
				Minor	NP	49:0	27:0	22:0
					AP	48:0	26:0	22:0
22	767.6	766.6	826.6				28:0	20:0
				Major	AH	50:1	30:0	20:1
				Minor	NP	51:0	29:0	22:0
23	793.6	792.6	852.6	Major	AH	50:1	30:0	20:1
				Minor	NP	51:0	29:0	22:0
					AP	50:0	30:0	20:0
24	795.6	794.6	854.6	Major	AH	50:0	28:0	22:0
				Minor	NP	52:0	30:0	22:0
25	807.6	806.6	866.6	Major	AH	50:0	28:0	22:0
				Minor	NP	52:0	30:0	22:0

Several fragments related to the fatty acyl chain were observed, including **a2**, **b2,c1**, **d2**, **e1**, and **e2**. Furthermore, **a3**, **a5**, and **f2** were fragment ions related to sphingoid unit. These results agree with the findings of t'Kindt et al. [12] and Shin et al. [24].

General MS/MS fragmentation pattern of A-type ceramides

Comparison of the MS/MS spectra of AS-, AdS-, AP-, and AH-type ceramides with different sphingoid units in the m/z region of the pseudomolecular ion of the MS/MS spectrum revealed characteristic patterns for AS-, AdS-, AP-, and AH-type ceramides (Fig. 3). The MS/MS spectrum of AS-type ceramides showed a series of fragment ion masses with differences of 18, 30, 32, and 48 Da, which originated from the loss of water, CH₂O group, methanol, and CH₂O and water, respectively, from their deprotonated pseudomolecular ions. The MS/MS spectrum of the AdS-type ceramide showed a series of fragment ion masses with differences of 18, 32, 48, and 66 Da, which originated from the loss of water, methanol, CH₂O and water, and CH₂O and two water molecules, respectively, from their pseudomolecular ions. The MS/MS spectrum of AP-type ceramide showed a series of fragment ion masses with differences of 18, 32, 36, and 48 Da, which originated from the loss of water, methanol, two water molecules, and CH₂O and water, respectively, from their pseudomolecular ions. The MS/MS spectrum of AH-type ceramide also showed characteristic fragment ion masses with differences of 18, 30, 36, 48, and 66 Da, which originated from the loss of water, CH₂O group, two water molecules, CH₂O and water, and CH₂O and two water molecules, respectively, from their pseudomolecular ions. Based on these informative and general MS/MS fragmentation patterns, we determined the sphingoid unit of A-type ceramides. These characteristic fragmentations of A-type ceramides differed from those of N-type ceramides [24]. For example, MS/MS spectra of AdS- and AH-type ceramides gave the fragment ion peak originated from the loss of CH₂O and two molecules of water, whereas those of NdS- and NH-type ceramides did not. The MS/MS spectra of AS- and AP-type ceramides gave specific fragment ion peak originated from the loss of methanol molecule and CH₂O and water molecule, respectively, whereas those of NS- and NP-type ceramides did not. The fragmentation patterns of A-type ceramides were also confirmed on A-type ceramides with different acyl chains (Fig. 4). Therefore, these patterns can be used to classify the sphingoid backbone of A-type ceramides in the human skin.

Identification of A-type ceramides in the stratum corneum of human skin

Direct infusion of lipid extracts into a tandem mass spectrometer has been used for ceramide profiling in various samples such as mouse liver [27], rat brain tissues and cerebral endothelial cells [25], human plasma [28], and human skin fibroblasts cell [29]. In our previous study, this method was applied to N-type ceramide analysis in the skin stratum corneum [24].

In this study, we identified A-type ceramides in the human stratum corneum using chip-based direct infusion nanoelectrospray-mass spectrometry. A typical mass spectrum of human stratum corneum extracts is shown in Fig. 5. MS³ spectra were produced from the product ion scan of the acetate adduct ion, and 25 A-type ceramides were identified based on the mass fragmentation patterns of A-type ceramides (Table 1). Some ions existed as A-type ceramide species, while other ions existed as AS/NH, AH/NP, or AdS/NP mixtures. In addition, analysis of the fragment ions revealed A-type ceramides that differed in amide-linked fatty acid and sphingoid carbon chain lengths. For example, an AP-type ceramide with a monoisotopic mass of 728.6 Da (41 carbon atoms) contained both the expected that most abundant ratio A23/S18 as well as A21/S20 and A25/S16.

Conclusions

In this study, the compound structures of the subspecies of four A-type ceramide classes (AS-, AdS-, AP-, and AH-type) were analyzed using chip-based direct infusion nanoelectrospray-ion trap MS. Based on the tandem mass fragmentation pattern of these ceramides, an A-type ceramide tandem mass library was generated (see ESM). We also applied the A-type ceramide MS/MS library to identify the structure of A-type ceramides extracted from the human stratum corneum using A-type ceramide-specific mass fragmentation patterns. Structural information for the A-type ceramide, including fatty acyl amide substituents and sphingoid groups, were obtained using direct infusion nanoelectrospray MS/MS in negative mode. This platform is useful for identifying biomarkers of various skin diseases such as atopic dermatitis, psoriasis, and allergic contact dermatitis.

Acknowledgments This work was supported by a grant from the Bio & Medical Technology Development Program of the National Research Foundation (NRF) funded by the Ministry of Science, ICT & Future Planning (grant no. NRF-2015M3A9E1028326 and NRF-2014R1A2A2A01002582), and the Korea Healthcare Technology R&D Project, Ministry of Health and Welfare (grant no. HN13C0076), Republic of Korea. The authors have no other relevant affiliations or financial involvement with any organization or entity with a financial interest in or financial conflict with the subject matter or materials discussed in the manuscript apart from those disclosed. No writing assistance was utilized in the production of this manuscript.

Compliance with ethical standards All individuals were enrolled with informed consent.

Conflict of interest The authors declare that they have no competing interests.

References

- Coderch L, Lopez O, de la Maza A, Parra JL. Ceramides and skin function. *Am J Clin Dermatol*. 2003;4:107–29.
- Huang HC, Chang TM. Ceramide 1 and ceramide 3 act synergistically on skin hydration and the transepidermal water loss of sodium lauryl sulfate-irritated skin. *Int J Dermatol*. 2008;47:812–9.
- Weerheim A, Ponc M. Determination of stratum corneum lipid profile by tape stripping in combination with high-performance thin-layer chromatography. *Arch Dermatol Res*. 2001;293:191–9.
- Mizutani Y, Mitsutake S, Tsuji K, Kihara A, Igarashi Y. Ceramide biosynthesis in keratinocyte and its role in skin function. *Biochimie*. 2009;91:784–90.
- Imokawa G, Akasaki S, Hattori M, Yoshizuka N. Selective recovery of deranged water-holding properties by stratum corneum lipids. *J Invest Dermatol*. 1986;87:758–61.
- Ishikawa J, Narita H, Kondo N, Hotta M, Takagi Y, Masukawa Y, et al. Changes in the ceramide profile of atopic dermatitis patients. *J Invest Dermatol*. 2010;130:2511–4.
- Janssens M, van Smeden J, Gooris GS, Bras W, Portale G, Caspers PJ, et al. Lamellar lipid organization and ceramide composition in the stratum corneum of patients with atopic eczema. *J Invest Dermatol*. 2011;131:2136–8.
- Imokawa G, Abe A, Jin K, Higaki Y, Kawashima M, Hidano A. Decreased level of ceramides in stratum corneum of atopic dermatitis: an etiologic factor in atopic dry skin? *J Invest Dermatol*. 1991;96:523–6.
- Lew BL, Cho Y, Kim J, Sim WY, Kim NI. Ceramides and cell signaling molecules in psoriatic epidermis: reduced levels of ceramides, PKC- α , and JNK. *J Korean Med Sci*. 2006;21:95–9.
- Motta S, Monti M, Sesana S, Caputo R, Carelli S, Ghidoni R. Ceramide composition of the psoriatic scale. *Biochim Biophys Acta*. 1993;1182:147–51.
- Masukawa Y, Narita H, Shimizu E, Kondo N, Sugai Y, Oba T, et al. Characterization of overall ceramide species in human stratum corneum. *J Lipid Res*. 2008;49:1466–76.
- fKindt R, Jorge L, Dumont E, Couturon P, David F, Sandra P, et al. Profiling and characterizing skin ceramides using reversed-phase liquid chromatography-quadrupole time-of-flight mass spectrometry. *Anal Chem*. 2012;84:403–11.
- Mutanu Jungersted J, Hellgren LI, Hogh JK, Drachmann T, Jemec GB, Agner T. Ceramides and barrier function in healthy skin. *Acta Derm Venereol*. 2010;90:350–3.
- Vietzke JP, Brandt O, Abeck D, Rapp C, Strassner M, Schreiner V, et al. Comparative investigation of human stratum corneum ceramides. *Lipids*. 2001;36:299–304.
- Thakoersing VS, van Smeden J, Mulder AA, Vreeken RJ, El Ghalbzouri A, Bouwstra JA. Increased presence of monounsaturated fatty acids in the stratum corneum of human skin equivalents. *J Invest Dermatol*. 2013;133:59–67.
- Uchida Y, Hara M, Nishio H, Sidransky E, Inoue S, Otsuka F, et al. Epidermal sphingomyelins are precursors for selected stratum corneum ceramides. *J Lipid Res*. 2000;41:2071–82.
- Lee YS, Choi KM, Choi MH, Ji SY, Yoo JM, Lee YM, et al. Simultaneous HPLC analysis of ceramide and dihydroceramide in human hairs. *Arch Pharm Res*. 2009;32:1795–801.
- Yano M, Kishida E, Muneyuki Y, Masuzawa Y. Quantitative analysis of ceramide molecular species by high performance liquid chromatography. *J Lipid Res*. 1998;39:2091–8.
- Samuelsson K, Sameulsson B. Gas chromatographic and mass spectrometric studies of synthetic and naturally occurring ceramides. *Chem Phys Lipids*. 1970;5:44–79.
- Joo KM, Nam GW, Park SY, Han JY, Jeong HJ, Lee SY, et al. Relationship between cutaneous barrier function and ceramide species in human stratum corneum. *J Dermatol Sci*. 2010;60:47–50.
- Farwanah H, Pierstorff B, Schmelzer CE, Raith K, Neubert RH, Kolter T, et al. Separation and mass spectrometric characterization of covalently bound skin ceramides using LC/APCI-MS and Nano-ESI-MS/MS. *J Chromatogr B Analyt Technol Biomed Life Sci*. 2007;852:562–70.
- Han X, Gross RW. Shotgun lipidomics: electrospray ionization mass spectrometric analysis and quantitation of cellular lipidomes directly from crude extracts of biological samples. *Mass Spectrom Rev*. 2005;24:367–412.
- Heiskanen LA, Suoniemi M, Ta HX, Tarasov K, Ekroos K. Long-term performance and stability of molecular shotgun lipidomic analysis of human plasma samples. *Anal Chem*. 2013;85:8757–63.
- Shin JH, Shon JC, Lee K, Kim S, Park CS, Choi EH, et al. A lipidomic platform establishment for structural identification of skin ceramides with non-hydroxyacyl chains. *Anal Bioanal Chem*. 2014;406:1917–32.
- Han X. Characterization and direct quantitation of ceramide molecular species from lipid extracts of biological samples by electrospray ionization tandem mass spectrometry. *Anal Biochem*. 2002;302:199–212.
- Hsu FF, Turk J, Stewart ME, Downing DT. Structural studies on ceramides as lithiated adducts by low energy collisional-activated dissociation tandem mass spectrometry with electrospray ionization. *J Am Soc Mass Spectrom*. 2002;13:680–95.
- Han X, Yang J, Cheng H, Ye H, Gross RW. Toward fingerprinting cellular lipidomes directly from biological samples by two-dimensional electrospray ionization mass spectrometry. *Anal Biochem*. 2004;330:317–31.
- Simons B, Kauhanen D, Sylvanne T, Tarasov K, Duchoslav E, Ekroos K. Shotgun lipidomics by sequential precursor ion fragmentation on a hybrid quadrupole time-of-flight mass spectrometer. *Metabolites*. 2012;2:195–213.
- Liebisch G, Drobnik W, Reil M, Trumbach B, Arnecke R, Olgemoller B, et al. Quantitative measurement of different ceramide species from crude cellular extracts by electrospray ionization tandem mass spectrometry (ESI-MS/MS). *J Lipid Res*. 1999;40:1539–46.